

Frequency evaluation of UTC(NPL) by NPL-E3Yb+3 for the period MJD 61069 to 61094

National Physical Laboratory

March 4, 2026

The secondary frequency standard NPL-E3Yb+3 and an optical frequency comb were used to evaluate the frequency of UTC(NPL) over a period of 25 days from MJD 61069 to MJD 61094 (29th January 2026 – 23rd February 2026). The Yb⁺ ion optical clock operation covers 87.43 % of the total measurement period. The result of the evaluation is reported in table 1 and is made using the CCTF 2021 recommended frequency value for the $4f^{14}6s\ ^2S_{1/2} - 4f^{13}6s^2\ ^2F_{7/2}$ unperturbed optical transition in $^{171}\text{Yb}^+$: 642 121 496 772 645.12 Hz with a relative standard uncertainty of $u_{\text{Srep}} = 1.9 \times 10^{-16}$ [1].

Table 1: Results of the evaluation of UTC(NPL) by NPL-E3Yb+3

Period of estimation	$y(\text{UTC}(\text{NPL}) - \text{NPL-E3Yb+3})/10^{-16}$	$u_A/10^{-16}$	$u_B/10^{-16}$	$u_{A/\text{Lab}}/10^{-16}$	$u_{B/\text{Lab}}/10^{-16}$	$u_{\text{Srep}}/10^{-16}$	Uptime
MJD 61069–61094	9.50	0.011	0.033	1.29	0.84	1.9	87.43 %

1 Measurement configuration

The operation of NPL-E3Yb+3 is described in section 2 of [2]. The electric octupole (E3) transition of $^{171}\text{Yb}^+$ was probed with a clock laser at 467 nm, frequency-doubled from 934 nm. The 934 nm laser was prestabilised to a local cavity and then further stabilised to a 1064 nm ultrastable laser [3] via an optical frequency comb. A feedback loop acting on an acousto-optic modulator (AOM) kept the clock laser frequency in resonance with the $^{171}\text{Yb}^+$ clock transition.

The optical frequency comb was used to measure the 934 nm laser frequency relative to the reference frequency of the comb, which was the unsteered output of the maser HM6. The steered output of HM6 was used to generate UTC(NPL). The frequency ratio between NPL-E3Yb+3 and the unsteered frequency from HM6 was therefore evaluated using the comb measurements of the 934 nm light and the AOM frequency corrections.

The offset between the steered and unsteered signals from HM6 was measured by a phase comparator throughout the measurement period. The model of TimeTech phase comparator has been changed since the last reported period (MJD 60944 - 60969). The previous model P&F Comp. 8 has now been replaced with TIM-10265, the key difference being that this new model measures 100 MHz signals instead of 10 MHz.

2 NPL-E3Yb+3 evaluation

Type A uncertainty

The type A uncertainty u_A is the statistical contribution from the frequency instability of NPL-E3Yb+3. This was estimated based on a white frequency noise component of $1.5 \times 10^{-15} / \sqrt{\tau}$ extrapolated to the duration of the evaluation period. This frequency instability is a conservative estimate, based on the Allan deviation of the frequency ratio with the local optical lattice clock NPL-Sr1 measured in November 2024. The probing parameters in November 2024 had a slightly higher QPN-limited instability than the parameters used for the measurement in the period MJD 61069–61094.

Type B uncertainty

The type B uncertainty u_B is the sum in quadrature of the systematic uncertainty of NPL-E3Yb+3 and the uncertainty of the relativistic redshift relative to the conventionally adopted reference potential $W_0 = 62\,636\,856.0 \text{ m}^2\text{s}^{-2}$.

The uncertainty evaluation of NPL-E3Yb+3 is described in [2], and the systematic frequency corrections and uncertainty budget for NPL-E3Yb+3 for the period of this report are given in table 2. The geopotential value for NPL-E3Yb+3 is evaluated based on the ion being 1.029(1) m above a reference marker in the floor of laboratory G4-L16. The geopotential of the reference marker is taken from [4].

Electric quadrupole shift

Since October 2024, the measurement of the electric quadrupole shift has been simplified and has become more direct. Previously, the E2 transition was probed in 5 alternating magnetic field directions in order to fit the electric field gradient and calculate the electric quadrupole shift in the y-direction, which is the quantisation axis direction used for probing the E3 transition. Changes in optical setups have enabled the direct probing of the E2 in the y-direction, reducing the required number of magnetic fields from 5 to 3, and allowing the direct measurement of the shift without the need for a fit.

The quadrupole shift was measured twice, once at the beginning and once at the end of the measurement period and the mean value of shift was taken. Conditions in the trap were demonstrated to have remained stable throughout the measurement period, as judged by periodic monitoring of the ion’s micromotion.

Table 2: Uncertainty budget for the Yb⁺ ion optical clock for this evaluation period. Reported uncertainties correspond to 68% confidence intervals. This table applies to the period MJD 61069–61094.

Systematic effect	Correction /10⁻¹⁸	Uncertainty /10⁻¹⁸
Black-body radiation	0	1.2
Servo offset	0	1.0
Electric quadrupole	-26.6	1.0
Quadratic Zeeman (DC)	29.1	0.7
Background gas collisions	0	0.6
Phase chirp	0	0.5
Second-order Doppler	1.7	0.4
AC Stark - probe beam	0	0.3
Trapping RF Stark	0.37	0.09
AC Stark - overshoot	-0.02	0.02
Quadratic Zeeman (AC)	0.01	0.02
Trap-induced AC Zeeman	-0.27	< 0.01
AC Stark - leakage light	< 0.01	< 0.01
Total correction	4.2	2.2
Relativistic redshift	-1186.9	2.5
Total including relativistic redshift	-1182.7	3.3

3 Frequency comparison

Type A uncertainty

The uncertainty $u_{A/\text{Lab}}$ arises mainly from the dead time in the comparison between HM6 and NPL-E3Yb+3, and includes both a deterministic correction due to maser drift and a stochastic contribution (table 3).

The analysis method for the deterministic downtime correction is described in detail in section 5.2.2 of [5]. The maser HM6 was drifting linearly throughout the measurement period. The deterministic downtime correction was calculated as the difference between the mean of the linear fit to the maser frequency during the uptime of NPL-E3Yb+3 and the mean of the linear fit during the entire measurement period MJD 61069–61094.

The stochastic contribution was estimated by a method described in reference [6]. This involves a Monte-Carlo approach where the frequency noise of HM6 is simulated 1000 times, with the standard deviation of the offsets providing an estimate for the frequency uncertainty arising from the dead times in the operation of NPL-E3Yb+3.

The maser noise model used comprised white phase noise of $3.90 \times 10^{-13} / \tau$, white frequency noise of $5.60 \times 10^{-14} / \sqrt{\tau}$, and a flicker frequency floor of 1.90×10^{-15} . In addition,

maser HM6 exhibits periodic frequency fluctuations that were estimated as an additional noise process proportional to the sum of four sinusoids in the simulated noise, with amplitudes 1.7×10^{-15} , 2.7×10^{-15} , 3.2×10^{-15} , 2.0×10^{-15} , and periods 3×10^3 s, 3×10^4 s, 8.64×10^4 s, and 1.728×10^5 s respectively. These values were derived from measurements of HM6 by NPL-E3Yb+3 during the evaluation period.

For this evaluation period, NPL-E3Yb+3 had an uptime of 87.43 %, distributed as shown in figure 1.

The TimeTech phase comparator that measures the offset between HM6 and UTC(NPL) introduces an additional contribution to $u_{A/\text{Lab}}$. This uncertainty is estimated by measuring the phase difference of UTC(NPL) referenced to itself with an equivalent TimeTech phase comparator of the same model.

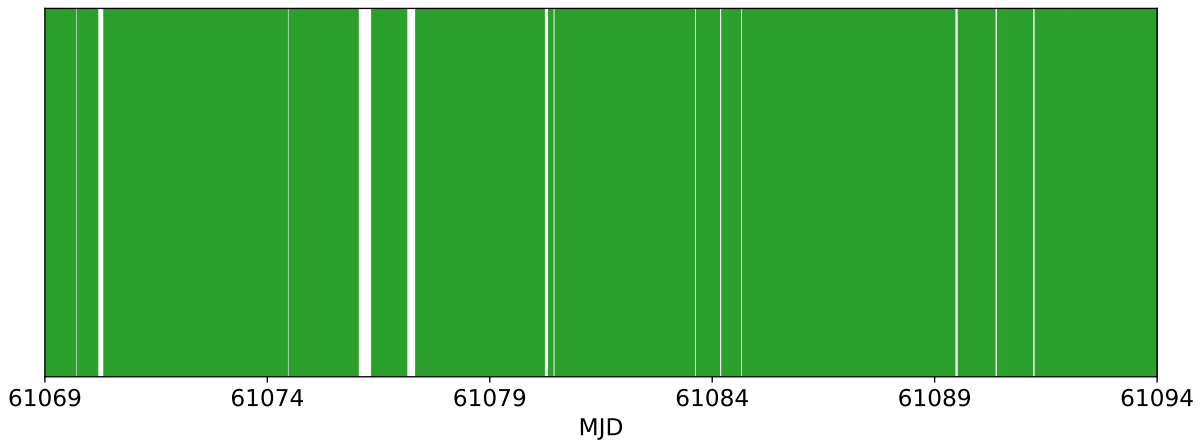


Figure 1: Uptime of NPL-E3Yb+3 over the evaluation period (green regions).

Contribution	Uncertainty / 10^{-18}
$u_{A/\text{Lab}}$ [Deterministic]	1
$u_{A/\text{Lab}}$ [Stochastic]	129
$u_{A/\text{Lab}}$ [HM6 - UTC(NPL)]	1
$u_{A/\text{Lab}}$[Total]	129

Table 3: A breakdown of the uncertainties included in $u_{A/\text{Lab}}$.

Type B uncertainty

The most significant contribution to the uncertainty $u_{B/\text{Lab}}$ is the distribution of the 10 MHz signal from HM6 to the frequency comb laboratory, and the subsequent synthesis in that laboratory of an 8 GHz signal against which the repetition rate of the frequency

comb was measured. Potential phase fluctuations were monitored using a loop-back comparison as described in reference [7], and their contribution to the uncertainty estimated from the mean frequency offset over the evaluation period.

The TimeTech phase comparator that measures the offset between HM6 and UTC(NPL) also contributes to $u_{\text{B/Lab}}$. This contribution is estimated based on the long-term instability of the phase difference of UTC(NPL) referenced to itself, measured with an equivalent TimeTech phase comparator of the same model.

Contribution	Uncertainty / 10^{-18}
$u_{\text{B/Lab}}$ [Distribution]	84
$u_{\text{B/Lab}}$ [HM6 - UTC(NPL)]	0.2
$u_{\text{B/Lab}}$[Total]	84

Table 4: A breakdown of the uncertainties included in $u_{\text{B/Lab}}$.

References

- [1] H S Margolis, G Panfilo, G Petit, C Oates, T Ido, and S Bize. The CIPM list ‘Recommended values of standard frequencies’: 2021 update. *Metrologia*, 61(3):035005, 2024.
- [2] A Tofful, C F A Baynham, E A Curtis, A O Parsons, B I Robertson, M Schioppo, J Tunesi, H S Margolis, R J Hendricks, J Whale, R C Thompson, and R M Godun. $^{171}\text{Yb}^+$ optical clock with 2.2×10^{-18} systematic uncertainty and absolute frequency measurements. *Metrologia*, 61(4):045001, 2024.
- [3] M. Schioppo, J. Kronjäger, A. Silva, R. Ilieva, J. W. Paterson, C. F.A. Baynham, W. Bowden, I. R. Hill, R. Hobson, A. Vianello, M. Dovale-Álvarez, R. A. Williams, G. Marra, H. S. Margolis, A. Amy-Klein, O. Lopez, E. Cantin, H. Álvarez Martínez, R. Le Targat, P. E. Pottie, N. Quintin, T. Legero, S. Häfner, U. Sterr, R. Schwarz, S. Dörscher, C. Lisdat, S. Koke, A. Kuhl, T. Waterholter, E. Benkler, and G. Grosche. Comparing ultrastable lasers at 7×10^{-17} fractional frequency instability through a 2220 km optical fibre network. *Nature Communications*, 13(1):212, 2022.
- [4] F. Riedel, A. Al-Masoudi, E. Benkler, S. Dörscher, V. Gerginov, C. Grebing, S. Häfner, N. Huntemann, B. Lipphardt, C. Lisdat, E. Peik, D. Piester, C. Sanner, C. Tamm, S. Weyers, H. Denker, L. Timmen, C. Voigt, D. Calonico, G. Cerretto, G. A. Costanzo, F. Levi, I. Sesia, J. Achkar, J. Guéna, M. Abgrall, D. Rovera, B. Chupin, C. Shi, S. Bilicki, E. Bookjans, J. Lodewyck, R. Le Targat, P. Delva, S. Bize, F. N. Baynes, C. F. A. Baynham, W. Bowden, P. Gill, R. M. Godun, I. R. Hill, R. Hobson, J. M. Jones, S. A. King, P. B. R. Nisbet-Jones, A. Rolland, S. L. Shemar, P. B. Whibberley, and H. S. Margolis. Direct comparisons of European primary and secondary frequency standards via satellite techniques. *Metrologia*, 57(4):045005, 2020.
- [5] A Tofful. *Advances in performance and automation of a single ytterbium ion optical clock*. PhD thesis, Imperial College London, 2023.
- [6] D.-H. Yu, M. Weiss, and T. E. Parker. Uncertainty of a frequency comparison with distributed dead time and measurement interval offset. *Metrologia*, 44(1):91, Feb 2007.
- [7] R. Hobson, W. Bowden, A. Vianello, A. Silva, C. F. A. Baynham, H. S. Margolis, P. E. G. Baird, P. Gill, and I. R. Hill. A strontium optical lattice clock with 1×10^{-17} uncertainty and measurement of its absolute frequency. *Metrologia*, 57(6):065026, Dec 2020.